Analyst

PAPER
Pak Kin Wong *et al.*
Electrokinetic focusing and separation of
mammalian cells in conductive biological fluids

Dynamic Article Links ▶

PAPER

Electrokinetic focusing and separation of mammalian cells in conductive biological fluids†

Jian Gao,[ab] **Reza Riahi,**[a] **Mandy L. Y. Sin,**[ac] **Shufeng Zhang**[d] **and Pak Kin Wong**[*a]

Active manipulation of cells, such as trapping, focusing, and isolation, is essential for various bioanalytical applications. Herein, we report a hybrid electrokinetic technique for manipulating mammalian cells in physiological fluids. This technique applies a combination of negative dielectrophoretic force and hydrodynamic drag force induced by electrohydrodynamics, which is effective in conductive biological fluids. With a three-electrode configuration, the stable equilibrium positions of cells can be adjusted for separation and focusing applications. Cancer cells and white blood cells can be positioned and isolated into specific locations in the microchannel under both static and dynamic flow conditions. To investigate the sensitivity of the hybrid electrokinetic process, AC voltage, frequency, and bias dependences of the cell velocity were studied systematically. The applicability of the hybrid electrokinetic technique for manipulating cells in physiological samples is demonstrated by continuous focusing of human breast adenocarcinoma spiked in urine, buffy coats, and processed blood samples with 98% capture efficiency.

Introduction

Microfluidics holds great promises in various biological and biomedical applications.[1,2] The ability to physically manipulate cells, such as focusing, trapping, and isolation, is often required to enhance the performance of microfluidic bioanalytical systems. For instance, cell focusing is performed in a microflow cytometer to position the target cells into the detection region.[3–6] Cell trapping can facilitate the investigation of cell–cell interaction, hybridoma production, and reprogramming of somatic cells.[7–9] Furthermore, cell separation is a fundamental microfluidic operation that is required in numerous diagnostic applications.[10–12] In particular, there is a strong interest recently to isolate exfoliated cancer cells from physiological samples, *e.g.*, urine and blood, due to its potential in early stage cancer diagnostics and drug treatment monitoring.[13–17] To isolate cancer cells in physiological samples, immunoaffinity-based techniques have been adapted to capture cells expressing specific surface biomarkers (*e.g.*, EpCAM).[17] Physical approaches, such as physical filtering and centrifugation, have also been adapted to separate cancer cells that do not express specific surface biomarkers.[18,19] However, physical separation approaches cannot isolate cells with similar properties and a significant number of white blood cells can be retained in the sample when physical separation techniques (*e.g.*, filtering) are applied for isolation of cancer cells. Therefore, novel mechanisms for manipulating cells in biological samples are highly desirable in cell separation and other lab-on-a-chip applications.

To actively manipulate cells in the microscale, magnetic, optical, hydrodynamic, acoustic, and electrokinetic forces are commonly applied in microfluidic bioanalytical systems.[20] Among these techniques, AC electrokinetics is one of the most promising approaches for developing fully integrated lab-on-a-chip systems due to the advantages of label-free manipulation, well-established techniques for fabricating microelectrodes, and low voltage requirement.[21–25] Several electrokinetic phenomena have been applied for cell manipulation.[26,27] For instance, electrophoresis (EP) directly manipulates cells depending on the charges on the cell surface and in the cytoplasm. Dielectrophoresis (DEP) is the motion of polarizable particles due to the interaction between the induced dipole and the inhomogeneous electric field.[28,29] The time averaged DEP force is given by $F_{DEP} = 2\pi R^3 \varepsilon \mathrm{Re}[K(\omega)]\nabla|E_{rms}|^2$, where R and ε are the radius of the cell and permittivity of the media, respectively. E_{rms} is the root-mean-square electric field. $\mathrm{Re}[K(\omega)]$ is the real part of the Clausius–Mossotti factor, which represents the effective polarization of the cell in the medium. Recently, several DEP-based cell manipulation devices have been developed for microfluidic

aDepartment of Aerospace and Mechanical Engineering, The University of Arizona, Tucson, Arizona 85721, USA. E-mail: pak@email.arizona.edu; Fax: +1-520-621-8191; Tel: +1-520-626-2215

bDepartment of Chemical Engineering, Shandong Polytechnic University, Jinan 250353, China

cDepartment of Urology, Stanford University, Palo Alto, California, 94304, USA

dDepartment of Physics, The University of Arizona, Tucson, Arizona 85721, USA

† Electronic supplementary information (ESI) available: Videos demonstrating separation of cancer cells in buffer, urine, and buffy coat samples under static and dynamic conditions. See DOI: 10.1039/c2an35707k

manipulation of cells, such as bacteria and cancer cells. For instance, DEP flow-field fractionation, lateral-driven DEP, electrodeless DEP, multi-frequency DEP, and traveling-wave DEP have been demonstrated for cell separation in microfluidic systems.[30–37] However, dilution and re-suspension of cells in working buffers are often required to enhance the effective cell polarization and to minimize the effect of electrohydrodynamics during DEP manipulation. Few works have been performed to investigate electrokinetic manipulation of cells in high-conductivity, physiological samples.[32,33]

Multiple electrokinetic phenomena can co-exist, since the involvement of Joule heating and electrokinetics-induced fluid motion is often unavoidable in electrokinetic manipulation of high-conductivity fluids. For example, external electric field can generate electrohydrodynamic fluid motion, such as AC electrothermal flow (ACEF) and AC electroosmosis (ACEO) with Faradaic charging.[38–44] The fluid motion exerts its effect on embedded cells *via* hydrodynamic drag, $F_{EH} \sim R^1$. The involvement of multiple electrokinetic phenomena simultaneously represents a fundamental challenge in understanding the observed electrokinetic effects and the influence of other electrokinetic phenomena is often neglected in DEP studies.[45] On the other hand, the co-existence of the electrokinetic phenomena creates new opportunities in combining multiple electrokinetic techniques, *i.e.*, hybrid electrokinetics.[46–49] With hybrid electrokinetics, the overall effectiveness of cell manipulation can be enhanced by taking advantage of the unique characteristics of each electrokinetic phenomenon. For example, the long-range electrohydrodynamics can potentially enhance the effective manipulation region of DEP, which rapidly decays from the electrode. We have demonstrated a hybrid electrokinetic bacteria concentrator that combines positive DEP and electrohydrodynamics for enhancing the trapping efficiency.[47] Furthermore, the dominance of a local particle trapping force and a fluid motion induced drag force is sensitive to the size of the cell and provides an effective mechanism for size-based particle separation. Nevertheless, little is known about hybrid electrokinetic manipulation of mammalian cells in conductive (typically on the order of 1 S m^{-1}) biological fluids, such as urine and buffy coats. Furthermore, the feasibility of using multiple electrokinetic forces for trapping and separating cancer cells in physiological samples has not been explored.

In this study, we report a hybrid electrokinetic technique to trap and isolate human breast adenocarcinoma (MDA-MB-231) from the sample matrix. While most DEP cell manipulation techniques require re-suspension of cells in low-conductivity working buffer, hybrid electrokinetics allows effective cell manipulation in high-conductivity, physiological samples including urine, buffy coats, and processed blood. Unlike our previous work in hybrid electrokinetic manipulation of bacteria,[47] which are trapped at the edges of the electrode due to positive DEP, cancer cells experience negative DEP and are pushed away from the electrodes depending on the electrode configuration. This opens new possibility in manipulating mammalian cells for various microfluidic operations. By optimizing the operating conditions, the relative strength between different forces can be adjusted to create a cell-specific force field for trapping and separation of cancer cells from urine and buffy coat samples.

Materials and methods

Device design

The system for studying hybrid electrokinetic cell manipulation consists of a set of three parallel electrodes integrated in a microchannel (Fig. 1a and b). In this design, cells experience negative DEP due to the high conductivity of the samples (~1 S m^{-1}) and are pushed away to regions with weak electric field strengths.[50–52] Numerical simulation (CFDRC-ACE) was performed to visualize the electric field distribution in the three-parallel-electrode configuration (Fig. 1c and d). Examining the electric field distribution reveals that the regions between the gap and on top of the center electrode have the weakest field strengths. To form a stable trap, the negative dielectrophoretic force can be balanced by other forces near the microelectrodes. For instance, cells experience hydrodynamic drag force induced by electrohydrodynamics and electrophoretic force, which are sensitive to the size and electrical properties of the cells. By optimizing the operating conditions, cells could be trapped in different equilibrium positions based on their physical properties.

Device fabrication

The electrodes for hybrid electrokinetic manipulation were fabricated by sputtering 150 nm titanium, 300 nm gold, and 150 nm titanium on a glass substrate and were patterned by lift-off. The Ti–Au–Ti electrode combination is chosen due to its stability during electrokinetic manipulation.[47] Unless otherwise specified, the length, width and distance of the electrodes were 2.5 mm, 50 μm and 125 μm respectively. The microfluidic channels were fabricated by molding polydimethylsiloxane (PDMS) with photoresist molds or laser machined structures. The glass substrate with microelectrodes was sealed with the PDMS microchannel by plasma treatment (PDC-001, Harrick Plasma). The fluid flow in the dynamic trapping experiment was regulated by a programmable syringe pump (NE-100, New Era Pump Systems, Inc. USA). A function generator (33120A, Hewlett Packard) was used to supply the voltage signals and the AC potential across the electrode was monitored with a digital oscilloscope (GDS-1102, GW Instek).

Cancer cells and physiological samples

The human mammary gland adenocarcinoma, MDA-MB-231, and HeLa cell lines were obtained from the American Type Culture Collection (ATCC, HTB-26). Cells were cultured in DMEM with 10% FBS, 1% L-glutamine and 0.1% gentamicin. The cells were seeded at 25–40% confluence and were maintained at 37 °C, 100% humidity, and 5% CO$_2$. Cells at passages 2 to 10 were used. Before the experiment, the cells were pre-stained using 3,3'-dihexyloxacarbocyanine iodide (DiOC6(3), Sigma) and incubated for 15 minutes at 37 °C in the dark. Then, the stained cells were washed 5 times with the growth medium to remove residual dyes prior to spiking into the sample. Human buffy coat and whole blood (WB) samples were obtained commercially (Innovative Research, IPLA-WB5 and IPLA-WB1). The lysed WB was prepared by adding red blood cell lysis buffer (Biolegend, USA) into WB and incubated for 15 min at 37 °C. The
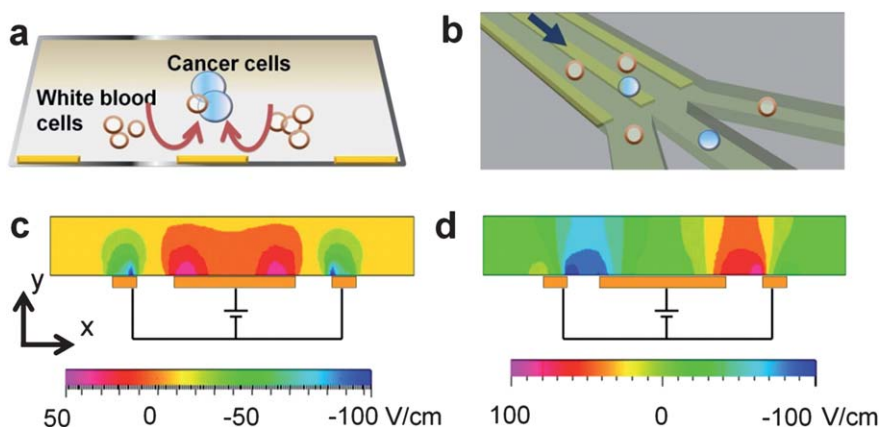
Fig. 1 (a) Cross-sectional view of the hybrid electrokinetic cell trapping device. Cancer cells and white blood cells are differentially trapped at different equilibrium locations inside the microchannel with the three-electrode design. Red arrows indicate electrokinetics-driven fluid motion in the spanwise direction. (b) Schematic view (3D) of the hybrid electrokinetic device. In this design, cancer cells and white blood cells are separated in the electrode region and delivered to different channels for downstream analysis. Blue arrows indicate the streamwise fluid motion driven by an external pump. (c and d) Computational fluid dynamics simulation of the (c) vertical (y direction) and (d) horizontal (x direction) components of the electric field for visualizing the low field region in the microchannel.

centrifuged WB was obtained by centrifuging WB for 10 min at 1000 rpm. The conductivities of the culture medium, buffy coat, lysed WB and centrifuged WB were approximately 1 S m^{-1} and the conductivity of the urine sample was 2.3 S m^{-1}.

Data collection and analysis

The motions of cells were observed with a digital inverted epi-fluorescence microscope (DMI 4000B, Leica Microsystems) equipped with a mercury lamp. Fluorescently stained cells were illuminated at 480 ± 40 nm and images were recorded at 527 ± 30 nm by a CCD camera and directly digitized into a video capture system. To estimate the capture efficiency, the number of the target cells passing through the outlet was counted by analyzing 300 consecutive images using image analysis software (ImageJ, NIH), and the efficiency was calculated based on the fraction of cell counts.[33]

Results

Hybrid electrokinetic cell focusing and separation

The behaviors of MDA-MB-231 and HeLa cells in culture media were first observed. With a combined DC and AC signal (7 Vpp at 100 kHz with 1.0 V DC bias) applied across the side and the center electrodes, the cells rapidly migrated and trapped on top of the center electrode. Under dynamic flow conditions, the cancer cells appear to be focused by a force field in the spanwise direction and are entrained with the fluid along the streamwise direction (ESI Movie 1†). To allow fluorescence observation behind the electrode, the cancer cells were pre-stained. The same trapping behavior was observed for unstained cells, suggesting that the dye does not alter the electrokinetic property of the cells. This is consistent with previous DEP based cell manipulation studies.[31–33] The focusing behavior was also observed in cancer cells spiked in urine. ESI Movie 2† shows spiked cancer cells in the downstream region of the channel. The same trapping behavior was observed in cells from passages 2 to 10. These

observations suggest that the hybrid electrokinetic technique is capable of focusing cancer cells in conductive buffers and urine samples.

The effects of electrokinetic trapping of MDA-MB-231 cells spiked in buffy coats were then investigated. Remarkably, MDA-MB-231 cells and white blood cells in the microchannel were observed to position into different equilibrium locations. In particular, the cancer cells migrated to the center electrode, while the majority of the white blood cells moved to areas between the gaps of the electrodes (Fig. 2a). Fluorescence microscopy verified that most cancer cells were captured on top of the center electrode (Fig. 2b). This differential cell trapping occurred under both static and dynamic flow conditions. The movement of cancer cells under static conditions is shown in Fig. 2c–e. ESI Movies 3 and 4† show cancer cells focused under static and dynamic conditions respectively. The same cell trapping behavior was also consistently observed when unlabeled cells were loaded into the channel separately. Therefore, the cell trapping does not require the existence of the other cells, and cancer cells can be separated from white blood cells based on their intrinsic properties.

Effects of the geometry of the electrode

The differential cell trapping is found to be sensitive to the electrode geometry and occurs only in specific configurations. Therefore, the effects of the electrode geometry, including the outer electrode width, gap distance, and inner electrode width, on the equilibrium positions for cell trapping were adjusted systematically. With a small gap (comparable to the size of the cell), only one equilibrium position on top of the center electrode, *i.e.*, cell focusing, was observed (Fig. 3a–c). All cells within the region are collected on top of the center electrode and focus into a line with a width of 10 μm. The effective capturing region extends approximately 100 μm from the gap of the electrode and is independent of the width of the outer electrode (Fig. 3a–c). Furthermore, the equilibrium position near the gap for cell
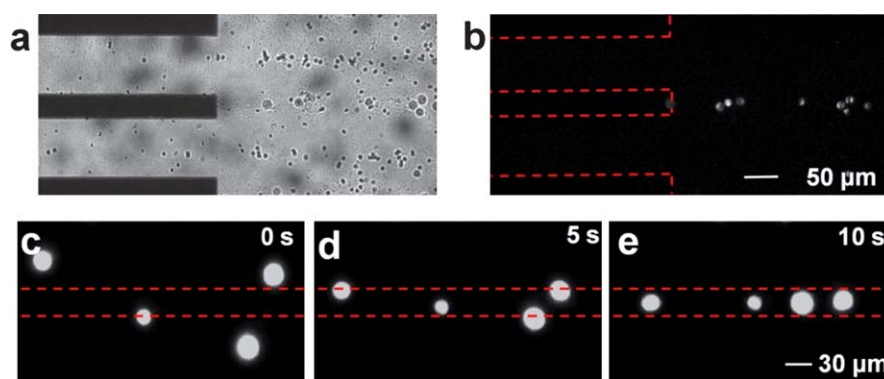
Fig. 2 (a and b) Bright field and fluorescence images showing the locations of cancer cells and white blood cells in the microchannel under dynamic (flow) conditions. Red dotted lines in (b) indicate the position of the electrodes. The fluid is moving from left to right. (c–e) Time lapse images for visualizing the movement of fluorescently labeled breast cancer cells under static conditions. The applied voltage was 7 Vpp at 100 kHz with 1.0 V DC offset.

trapping depends on the gap distance. Increasing the gap distance creates cell trapping equilibrium positions between the electrodes (Fig. 3d–f). The focusing width of white blood cells was observed to increase with the gap distance. Similarly, the trapping of cancer cells on top of the center electrode is sensitive to the width of the center electrode (Fig. 3g–i). With a large width of the center electrode, cells are trapped on top of the center electrode. The focusing width increases with the center electrode width. The equilibrium position on top of the center electrode vanishes if the center electrode width is small compared to the cell. Collectively, these results suggest that the equilibrium positions for cell focusing and separation are sensitive to the electrode geometry and can be tailored for different cell manipulation purposes, such as focusing and separation.

Characteristics of hybrid electrokinetics

To further investigate the cell trapping technique, the velocities of cancer cell migration toward the center electrode with different AC voltages, DC biases and frequencies were determined systematically. Fig. 4a shows the voltage dependence of the velocity of cancer cells at different locations in the microchannel. The velocity is highest in the region near the side electrode and decreases as the cell approaching the equilibrium position on top of the center electrode. The velocity generally increases with the applied voltage and shows a scaling exponent between 1.76 and 1.90, which is slightly lower than the exponent, 2, for DEP ($F_{DEP} \sim V^2$) (Fig. 4b). EP and electrohydrodynamics have different voltage dependences ($F_{EP} \sim V^1$; $F_{ACEF} \sim V^4$; $F_{ACEO} \sim e^{v/v_0}$), which suggests that the trapping force is primarily
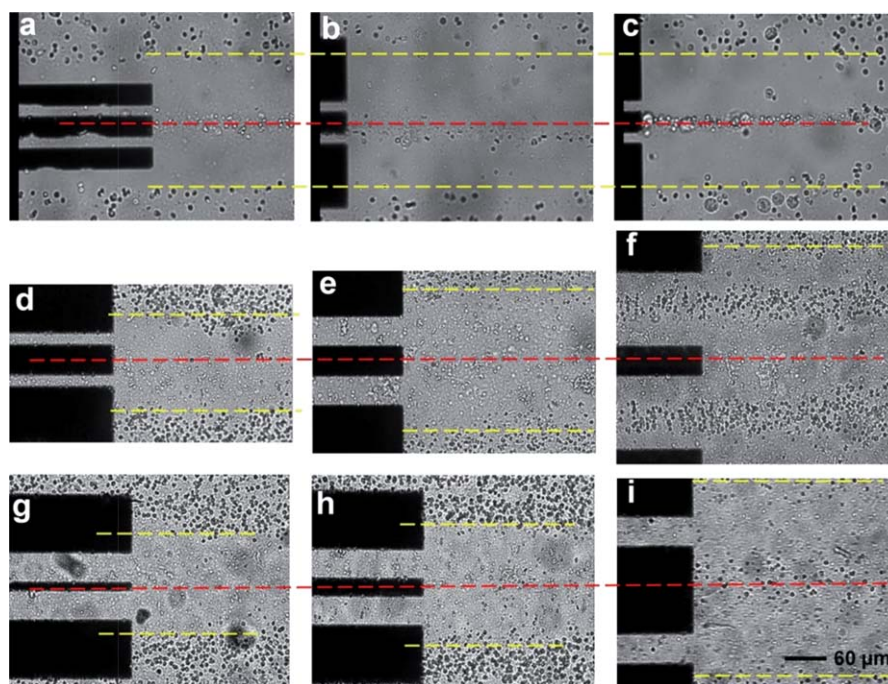

Fig. 3 Dependences of hybrid electrokinetic cell trapping on the (a–c) width of the outer electrode, (d–f) gap distance, and (g–i) width of the center electrode. Buffy coats spiked with MDA-MB-231 cells were tested. The fluid is moving from left to right. Dark areas are electrodes. Dotted lines indicate the effective cell capturing regions and the equilibrium position on top of the center electrode.
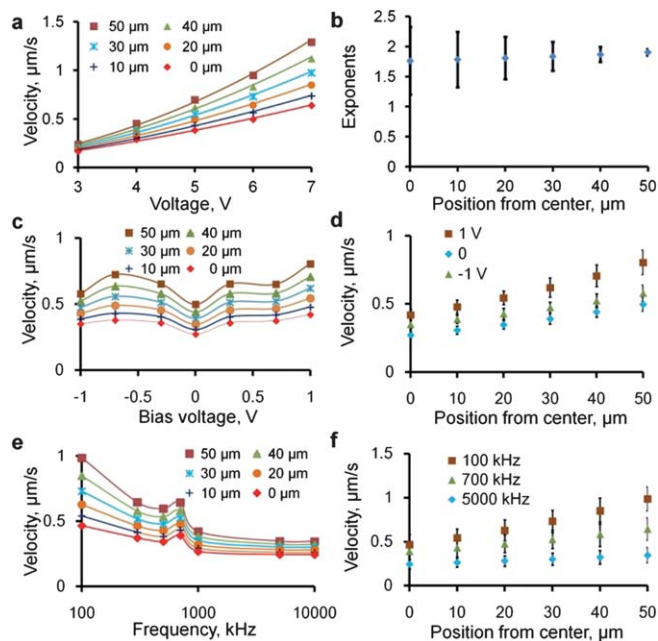
Fig. 4 (a) Voltage dependence of the cell velocity at different locations from the center electrode (*i.e.*, 0 μm is the equilibrium position). (b) Power dependence of the voltage on the cell velocity. (c) Bias voltage dependence on the cell velocity. (d) Comparison of the cell trapping velocity with different DC offsets. (e) Frequency dependence of the cell velocity. (f) Distribution of cell velocity at different frequencies.

driven by DEP. Nevertheless, the cell velocity could also be affected by other electrokinetic effects. For example, the involvement of EP should not be neglected. A DC bias on the AC potential increases the cell velocity by ~50% due to the existence of EP (Fig. 4c and d). Interestingly, negative bias also increases the cell velocity, while a positive bias shows a stronger enhancement effect. This observation suggests the involvement of electrohydrodynamics, which can be enhanced by both positive and negative bias voltages due to the nonlinearity of electrohydrodynamics.[38,41] The cell velocity with −1 V negative bias is ~10% higher than the value without the dc offset. The existence of electrohydrodynamics is further evidenced by observing the fluid circulation near the electrode with small cell debris and tracer particles that experience weaker DEP. Moreover, the cell velocity displays a strong dependence on the frequency (Fig. 4e and f). The frequency dependence can be understood by the polarization of the cell and is in general agreement with the result obtained from electrorotation and DEP field-flow fractionation.[50–52] Therefore, our data reveal that the cell trapping force is primarily driven by DEP and is enhanced by electrohydrodynamics and EP.

Hybrid electrokinetic manipulation of physiological samples

The operation of hybrid electrokinetics for cell trapping was further tested under different flow conditions and with different physiological samples. The numbers of cancer cells and white blood cells passing through the outlet were counted by analyzing images to estimate the capture efficiency. Fig. 5a shows the capturing efficiency, *i.e.*, the percentage of cells being captured

on the center electrode, of cancer cells in buffy coat with different flow rates. Below 0.1 μl min⁻¹, over 98% cancer cells were trapped on top of the center electrode while the majority of white blood cells (80–90%) were removed from the center region. A higher flow rate, however, could reduce the residual time of the cancer cell in the channel, thus the capturing efficiency. To explore separation of cancer cells from physiological samples, cancer cells were spiked in urine and blood samples diluted with red blood cell lysing buffer (Biolegend, USA) or centrifuged for 10 min at 1000 rpm. To compare the trapping effects under different conditions, the flow rate was maintained at 0.08 μl min⁻¹. Based on the result, the device shows comparable capturing efficiencies for buffy coat and urine (Fig. 5b). The capture efficiency, however, decreases slightly (<10%) for diluted and centrifuged blood samples. The decrease in the efficiency is conceivably due to the difference in viscosity and can be improved by reducing the flow rate, increasing the channel length, or multiplexing the microchannels.

Discussion

In this study, we demonstrate a hybrid electrokinetic technique for directly manipulating mammalian cells in conductive biological fluids. This is the first study that combines the three-electrode configuration and hybrid electrokinetics for mammalian cell manipulation. The principle for manipulating mammalian cells is fundamentally different from our previous work for concentrating bacteria that experience positive DEP, and the target bacteria are trapped at the edges of the center electrode. In this study, cancer cells and white blood cells experience negative DEP, which pushes the cells away to regions with weak electric field strength. By proper design of the device, mammalian cells can be focused on the top of the center electrode with a focusing width comparable to the size of the cell. Hybrid electrokinetic cell focusing could potentially be applied in applications such as microfluorescence-activated cell sorting or flow cytometry.

The cell trapping phenomena can be understood by the balance between negative DEP and other forces. For cancer cells, the equilibrium position exists on top of the center electrode. In the vertical direction, cells are pushed away by both DEP and the drag force, which are balanced by the gravitational force. The strong horizontal component of DEP traps the cancer cells on top of the center electrode (Fig. 1d). Since white blood cells have a smaller size and a weaker polarizability compared to cancer cells at this frequency,[50,51] the white blood cells are not stable on top of the center electrode and are entrained by the fluid motion.
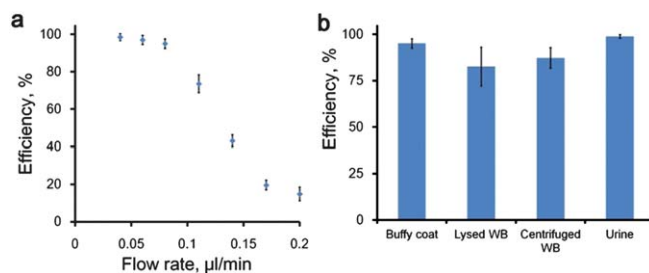

Fig. 5 (a) Dependence of the cancer cell capturing efficiency on the fluid flow rate. (b) Capturing efficiencies of cancer cells in buffy coat, lysed whole blood, centrifuged whole blood and urine.

In the gap region, the negative DEP force experienced by the white blood cells is balanced by the electrophoretic force and the hydrodynamic drag induced by electrohydrodynamics, which circulates on top of the electrode and pushes the cells toward the center electrode (Fig. 1a). Therefore, separation of cancer cells and white blood cells is due to the differences in their sizes ($F_{EH} \sim R$; $F_{DEP} \sim R^3$) and the effective polarization at the applied frequency. Notably, the equilibrium positions near the gap disappear and the white blood cells move to the center electrode when the microchannel is flipped up-side-down. This observation suggests the involvement of gravitational force, F_{grav}, and the cell trapping is the result of a tight balance between DEP and other forces. The dedicated balance between different forces, which are sensitive to the size and electrical properties of the cells, creates cell-specific force fields for trapping and isolation of cancer cells. The involvement of multiple forces in cell trapping is also evidenced by the dependence on the electrode geometry. Since the negative DEP force is only effective near the electrode edge, the focusing width of the equilibrium positions can be tuned by the width of the center electrode and the gap distance, as shown in Fig. 3. The electrode configuration, *i.e.*, the electric field distribution, provides a simple mechanism for turning the force field for cell focusing and cell separation. By adjusting the electrode configuration, the equilibrium positions near the gap can be modified for cell trapping and separation.

Conclusions

In summary, we have demonstrated a hybrid electrokinetic technique that is capable of selective trapping and separation of mammalian cells. In the future, theoretical and computational analyses should be performed to evaluate the relative strength of each forces and to guide the design of the hybrid electrokinetic device for other cell manipulation applications. While hybrid electrokinetics does not directly handle unprocessed whole blood, the ability to separate the cancer cell lines from white blood cells could potentially be applied for capturing exfoliated cancer cells in physiological samples by integrating with a size-based separator or other separation approaches (*e.g.*, *in situ* mixing with red blood lysis buffer which selectively lysed RBCs or pre-processed by centrifugation). Evaluating the device with clinical samples from patients should be performed to explore this feasibility. The throughput and efficiency of the system can be improved by increasing the residual time of the cells in the channel (*e.g.*, increasing the channel length). Furthermore, multiplexed microfluidic devices can also be developed by taking advantage of the parallel processing nature of microfabrication to increase the throughput of the systems. With the simplicity and effectiveness in conductive biological fluids, hybrid electrokinetics is envisioned to provide a useful approach for cell manipulation toward the development of novel biosensing systems in the future.

Acknowledgements

Notes and references

1 G. M. Whitesides, *Nature*, 2006, **442**, 368–373.
2 W. Yang and A. T. Woolley, *JALA*, 2010, **15**, 198–209.
3 G. Goddard, J. C. Martin, S. W. Graves and G. Kaduchak, *Cytometry, Part A*, 2006, **69**, 66–74.
4 J. Oakey, R. W. Applegate, E. Arellano, D. Di Carlo, S. W. Graves and M. Toner, *Anal. Chem.*, 2010, **82**, 3862–3867.
5 T. H. Wang, Y. H. Peng, C. Y. Zhang, P. K. Wong and C. M. Ho, *J. Am. Chem. Soc.*, 2005, **127**, 5354–5359.
6 Y. H. Lin and G. B. Lee, *Biosens. Bioelectron.*, 2008, **24**, 572–578.
7 A. O. Ogunniyi, C. M. Story, E. Papa, E. Guillen and J. C. Love, *Nat. Protoc.*, 2009, **4**, 767–782.
8 J. Wang and C. Lu, *Appl. Phys. Lett.*, 2006, **89**, 234102.
9 A. M. Skelley, O. Kirak, H. Suh, R. Jaenisch and J. Voldman, *Nat. Methods*, 2009, **6**, 147–152.
10 S. L. Stott, C. H. Hsu, D. I. Tsukrov, M. Yu, D. T. Miyamoto, B. A. Waltman, S. M. Rothenberg, A. M. Shah, M. E. Smas, G. K. Korir, F. P. Floyd, A. J. Gilman, J. B. Lord, D. Winokur, S. Springer, D. Irimia, S. Nagrath, L. V. Sequist, R. J. Lee, K. J. Isselbacher, S. Maheswaran, D. A. Haber and M. Toner, *Proc. Natl. Acad. Sci. U. S. A.*, 2010, **107**, 18392–18397.
11 D. W. Inglis, R. Riehn, R. H. Austin and J. C. Sturm, *Appl. Phys. Lett.*, 2004, **85**, 5093–5095.
12 L. R. Huang, E. C. Cox, R. H. Austin and J. C. Sturm, *Science*, 2004, **304**, 987–990.
13 S. Nagrath, L. V. Sequist, S. Maheswaran, D. W. Bell, D. Irimia, L. Ulkus, M. R. Smith, E. L. Kwak, S. Digumarthy, A. Muzikansky, P. Ryan, U. J. Balis, R. G. Tompkins, D. A. Haber and M. Toner, *Nature*, 2007, **450**, 1235–1239.
14 A. Murali, L. Kasman and C. Voelkel-Johnson, *BMC Cancer*, 2011, **11**, 168.
15 K. Yoshida, T. Sugino, H. Tahara, A. Woodman, J. Bolodeoku, V. Nargund, G. Fellows, S. Goodison, E. Tahara and D. Tarin, *Cancer*, 1997, **79**, 362–369.
16 S. L. Stott, R. J. Lee, S. Nagrath, M. Yu, D. T. Miyamoto, L. Ulkus, E. J. Inserra, M. Ulman, S. Springer, Z. Nakamura, A. L. Moore, D. I. Tsukrov, M. E. Kempner, D. M. Dahl, C. L. Wu, A. J. Iafrate, M. R. Smith, R. G. Tompkins, L. V. Sequist, M. Toner, D. A. Haber and S. Maheswaran, *Sci. Transl. Med.*, 2010, **2**, 25ra23.
17 M. Yu, S. Stott, M. Toner, S. Maheswaran and D. A. Haber, *J. Cell Biol.*, 2011, **192**, 373–382.
18 H. K. Lin, S. Zheng, A. J. Williams, M. Balic, S. Groshen, H. I. Scher, M. Fleisher, W. Stadler, R. H. Datar, Y. C. Tai and R. J. Cote, *Clin. Cancer Res.*, 2010, **16**, 5011–5018.
19 S. Zheng, H. Lin, J. Q. Liu, M. Balic, R. Datar, R. J. Cote and Y. C. Tai, *J. Chromatogr., A*, 2007, **1162**, 154–161.
20 D.-H. Kim, P. K. Wong, J. Park, A. Levchenko and Y. Sun, *Annu. Rev. Biomed. Eng.*, 2009, **11**, 203–233.
21 A. Ramos, H. Morgan, N. G. Green and A. Castellanos, *J. Phys. D: Appl. Phys.*, 1998, **31**, 2338–2353.
22 P. K. Wong, T. H. Wang, J. H. Deval and C. M. Ho, *IEEE-ASME Transactions on Mechatronics*, 2004, **9**, 366–376.
23 M. L. Sin, J. Gao, J. C. Liao and P. K. Wong, *J. Biol. Eng.*, 2011, **5**, 6.
24 R. Hart, E. Ergezen, R. Lec and H. Noh, *Biosens. Bioelectron.*, 2011, **26**, 3391–3397.
25 S. C. Wang, H. P. Chen, C. Y. Lee, C. C. Yu and H. C. Chang, *Biosens. Bioelectron.*, 2006, **22**, 563–567.
26 J. Voldman, *Annu. Rev. Biomed. Eng.*, 2006, **8**, 425–454.
27 E. D. Pratt, C. Huang, B. G. Hawkins, J. P. Gleghorn and B. J. Kirby, *Chem. Eng. Sci.*, 2011, **66**, 1508–1522.
28 H. A. Pohl, *J. Appl. Phys.*, 1951, **22**, 869–871.
29 R. Pethig, *Biomicrofluidics*, 2010, **4**, 022802.
30 P. R. C. Gascoyne, J. Noshari, T. J. Anderson and F. F. Becker, *Electrophoresis*, 2009, **30**, 1388–1398.
31 H. S. Moon, K. Kwon, S. I. Kim, H. Han, J. Sohn, S. Lee and H. I. Jung, *Lab Chip*, 2011, **11**, 1118–1125.
32 K. H. Han and A. B. Frazier, *Lab Chip*, 2008, **8**, 1079–1086.
33 S. Park, Y. Zhang, T. H. Wang and S. Yang, *Lab Chip*, 2011, **11**, 2893–2900.
34 T. Braschler, N. Demierre, E. Nascimento, T. Silva, A. G. Oliva and P. Renaud, *Lab Chip*, 2008, **8**, 280–286.
35 Y. J. Zhao, U. C. Yi and S. K. Cho, *J. Microelectromech. Syst.*, 2007, **16**, 1472–1481.

36 M. Hashimoto, H. Kaji and M. Nishizawa, *Biosens. Bioelectron.*, 2009, **24**, 2892–2897.

37 A. P. Brown, W. B. Betts, A. B. Harrison and J. G. O'Neill, *Biosens. Bioelectron.*, 1999, **14**, 341–351.

38 N. G. Green, A. Ramos, A. Gonzalez, A. Castellanos and H. Morgan, *J. Electrost.*, 2001, **53**, 71–87.

39 A. Castellanos, A. Ramos, A. Gonzalez, N. G. Green and H. Morgan, *J. Phys. D: Appl. Phys.*, 2003, **36**, 2584–2597.

40 M. L. Y. Sin, V. Gau, J. C. Liao and P. K. Wong, *JALA*, 2010, **15**, 426–432.

41 W. Y. Ng, S. Goh, Y. C. Lam, C. Yang and I. Rodriguez, *Lab Chip*, 2009, **9**, 802–809.

42 D. Lastochkin, R. H. Zhou, P. Wang, Y. X. Ben and H. C. Chang, *J. Appl. Phys.*, 2004, **96**, 1730–1733.

43 V. Studer, A. Pepin, Y. Chen and A. Ajdari, *Analyst*, 2004, **129**, 944–949.

44 M. L. Y. Sin, T. T. Liu, J. D. Pyne, V. Gau, J. C. Liao and P. K. Wong, *Anal. Chem.*, 2012, **84**, 2702–2707.

45 C. Meinhart, D. Z. Wang and K. Turner, *Biomed. Microdevices*, 2003, **5**, 139–145.

46 P. K. Wong, C. Y. Chen, T. H. Wang and C. M. Ho, *Anal. Chem.*, 2004, **76**, 6908–6914.

47 J. Gao, M. L. Y. Sin, T. Liu, V. Gau, J. C. Liao and P. K. Wong, *Lab Chip*, 2011, **11**, 1770–1775.

48 M. L. Y. Sin, Y. Shimabukuro and P. K. Wong, *Nanotechnology*, 2009, **20**, 165701.

49 M. L. Y. Sin, V. Gau, J. C. Liao, D. A. Haake and P. K. Wong, *J. Phys. Chem. C*, 2009, **113**, 6561–6565.

50 P. R. C. Gascoyne, X. B. Wang, Y. Huang and F. F. Becker, *IEEE Trans. Ind. Appl.*, 1997, **33**, 670–678.

51 J. Yang, Y. Huang, X. B. Wang, F. F. Becker and P. R. C. Gascoyne, *Anal. Chem.*, 1999, **71**, 911–918.

52 F. Yang, X. M. Yang, H. Jiang, P. Bulkhaults, P. Wood, W. Hrushesky and G. R. Wang, *Biomicrofluidics*, 2010, **4**, 13204.